Corrigan et al, http://www.jcb.org/cgi/content/full/jcb.201401072/DC1

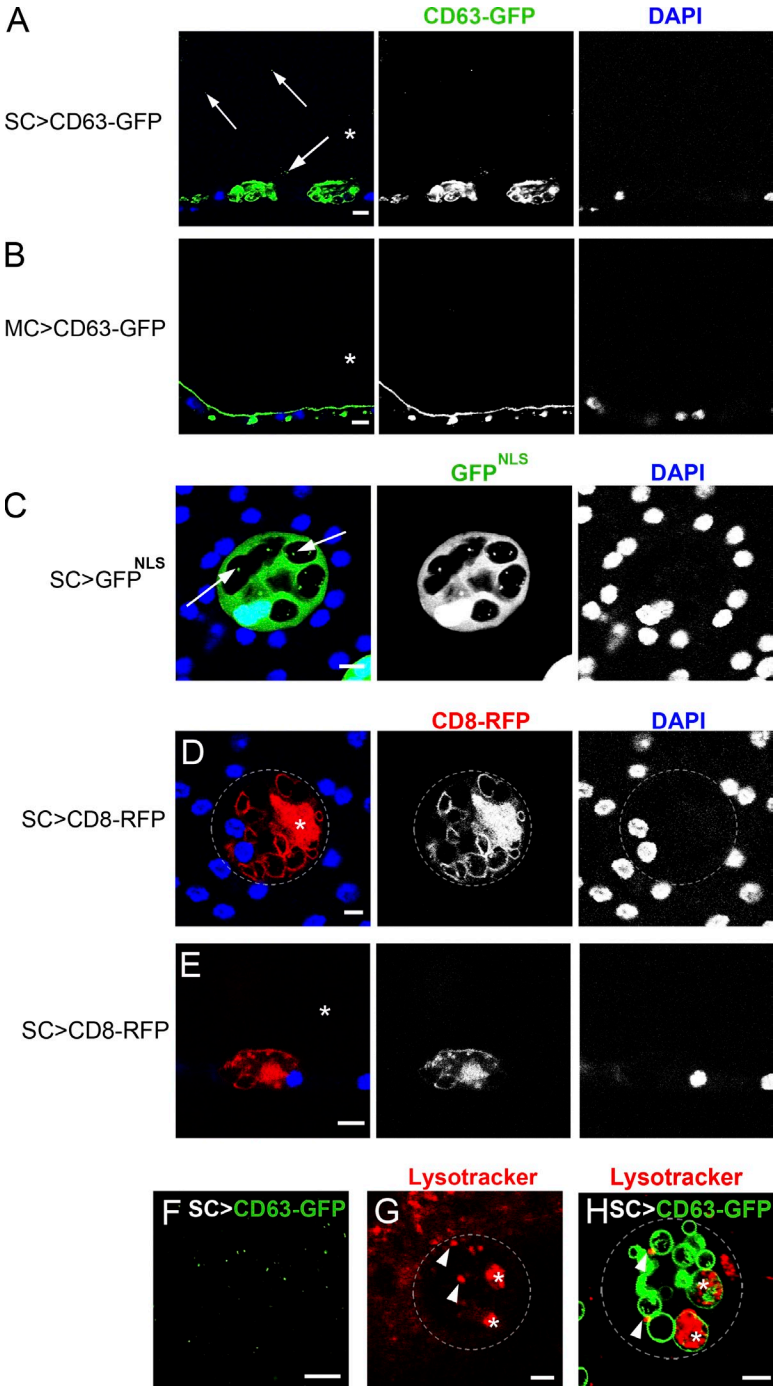

Figure S1. **SCs and not MCs secrete CD63-positive puncta.** (A and B) Transverse sections of AG (in an equivalent focal plane to Fig. 1 C) showing that CD63-GFP is secreted in puncta (arrows; see F for higher magnification image at higher gain setting) into the AG lumen (asterisks) when expressed by SCs (A) but not MCs, imaged here in the middle of the gland where no SCs are present (B). (C) Puncta containing cytoplasmic GFP can also occasionally be seen inside SC vacuoles (arrows) in the surface section. (D and E) CD8-RFP localizes either within (asterisk in D) or at the limiting membrane of large vacuoles (surface section in D) but is not secreted into the AG lumen (asterisk, transverse section in E). (F) Many CD63-GFP–positive puncta secreted by SCs into the AG lumen are detected when the sensitivity and resolution of confocal imaging is increased. (G and H) The w^{1118} (non-GFP marked) control SC (G), imaged live, contains two large (>2 µm, asterisks) and several small (<2 µm, arrowheads) acidic compartments, which stain strongly with LysoTracker red, similar to CD63-GFP–expressing SCs (H). Accurately counting these compartments is not possible because their limiting membranes are not marked. All images show SCs from 3-d-old males incubated at 28.5°C after eclosion. Fixed cell nuclei are stained with DAPI. Approximate outline of cell is marked in D, G, and H. Bars: (A, B, and F) 10 µm; (C–E, G, and H) 5 µm.

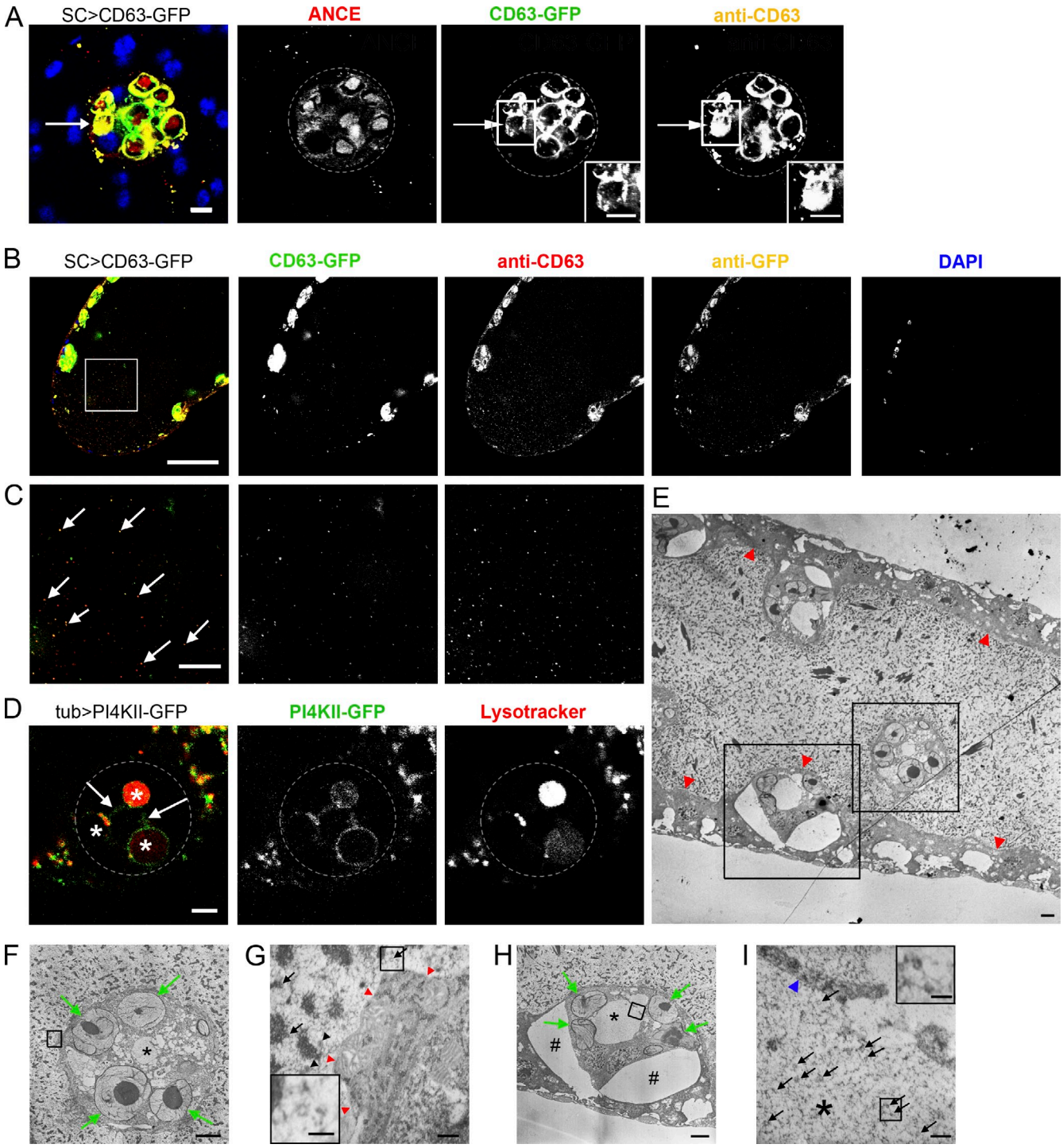

Figure S2. **SCs have large acidic compartments containing internalized CD63-GFP.** (A) A CD63-GFP–expressing SC stained with anti-ANCE and anti-CD63 antibodies reveals one compartment that is filled with CD63 but has low GFP fluorescence (arrows; insets show higher magnification images of boxed regions that include this compartment). This compartment does not contain a dense ANCE core (arrows). (B and C) Transverse section through the lumen of an AG containing CD63-GFP–expressing SCs stained with anti-CD63 and anti-GFP antibodies. Many CD63-GFP fluorescent puncta in the AG lumen colocalize with the anti-CD63 antibody (e.g., arrows in C). C is a higher magnification image of the square outlined in B. (D) Live image of an SC from a *tub-PI4KII-GFP* fly stained with LysoTracker. The late endosome and lysosome marker PI4KII localizes to the limiting membrane of large acidic compartments (asterisks) as well as tubulations extending between them (arrows), which have been observed previously in *Drosophila* salivary gland cells (Burgess et al., 2012). (E–I) Electron micrographs of virgin w^{1118} male AGs. MCs (apical membranes marked with red arrowheads in E) make up the majority of the monolayered epithelium; SCs (boxed in E) are dispersed between MCs, bulge into the lumen, and can be seen in transverse (e.g., cell in H) or surface (e.g., cell protruding into lumen in F) section. SCs contain SVs, comprising an electron-dense core and fibrillar material (F and H, green arrows) and one or two large and less electron-dense, non-SV compartments (F and H, asterisks; H shown at high magnification in I), which by a process of elimination, must represent the large acidic compartments seen in live confocal imaging. The AG lumen contains a range of secreted structures (E), including putative membrane-bound vesicles (G, closed arrows and arrowheads; red arrowheads mark apical surface of epithelium), some of which (G, closed arrows; boxed area enlarged in inset) resemble the ~40-nm vesicles (I, arrows; enlarged in inset) observed inside the large multivesicular compartments in SCs (I, asterisk). These compartments therefore appear to be the counterparts of much smaller mammalian MVBs. F and H are higher magnification images of the boxed regions in E; G and I show higher magnification images of the regions boxed in F and H, respectively. All images show SCs from 3-d-old males incubated at 28.5°C after eclosion. Note that despite attempting several fixation protocols, we were unable to prevent spaces forming at high frequency between SC and MC plasma membranes in the epithelium (# in H). Preservation of compartment membranes was also not optimal (e.g., blue arrowhead in I). Approximate outline of cell is marked in A and D. Bars: (A [main images and insets] and D) 5 µm; (B) 50 µm; (C) 10 µm; (E, F, and H) 2 µm; (G and I, main images) 200 nm; (G and I, insets) 100 nm.

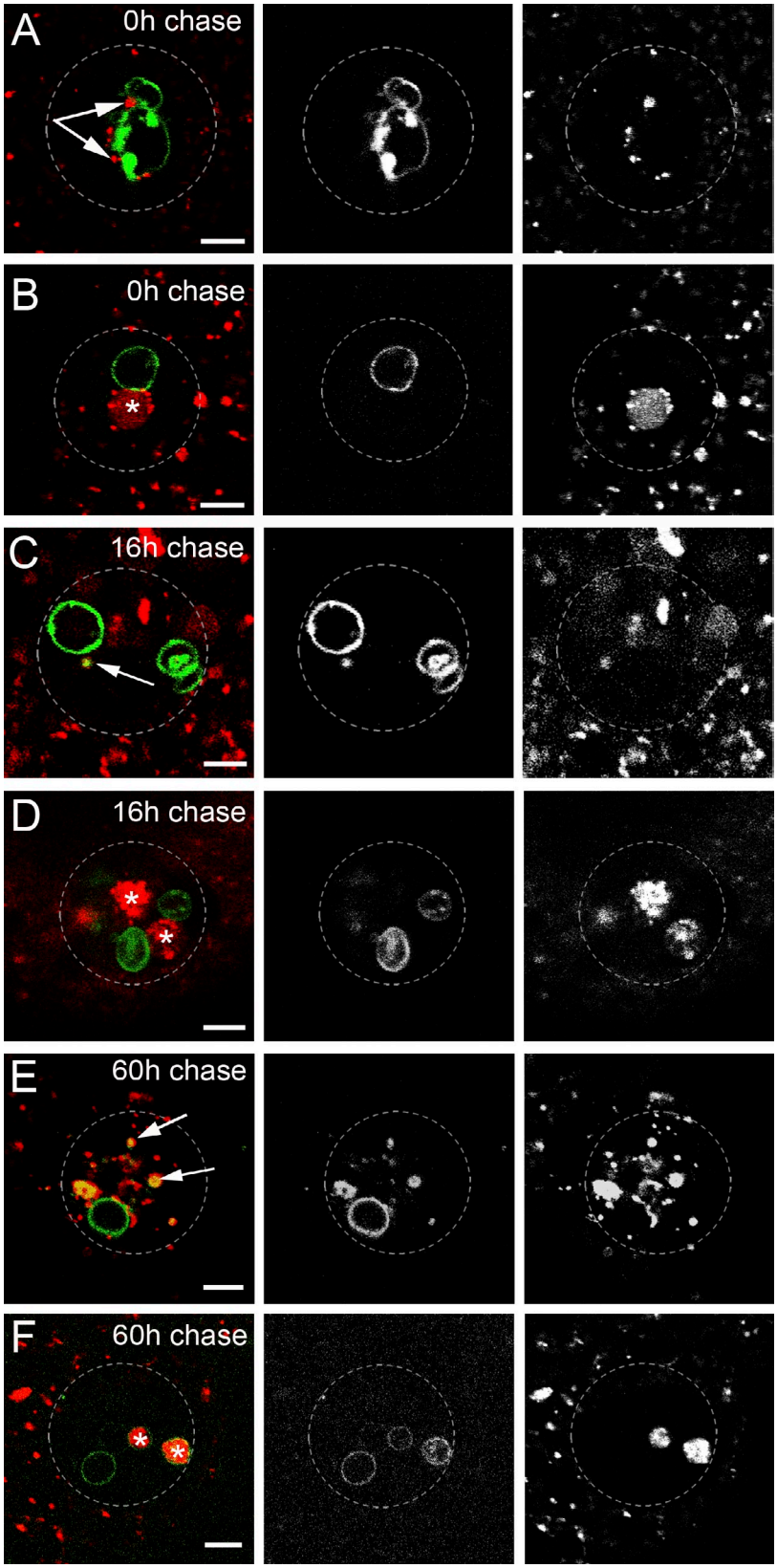

Figure S3. **Analysis of CD63-GFP trafficking and internalization in mMVBLs.** Images from Fig. 3 showing individual color channels: an 8-h pulse of CD63-GFP (induced by inhibition of GAL80^{ts} at 28.5°C) was chased at 18°C for 0–60 h, and proportions of cells with one or more LysoTracker red–positive iLEs (arrows in A, C, and E) and mMVBLs (asterisks in B, D, and F), which were CD63-GFP positive, were determined. The rate of CD63 traffic into endolysosomes is not identical in all cells (Fig. 3 G). Note that when the temperature is shifted down at the end of the pulse, transcripts encoding CD63-GFP are not immediately degraded, so new protein will continue to be made, potentially explaining the persistence of GFP fluorescence in SVs and iLEs. Approximate outline of cell is marked. Bars, 5 µm.

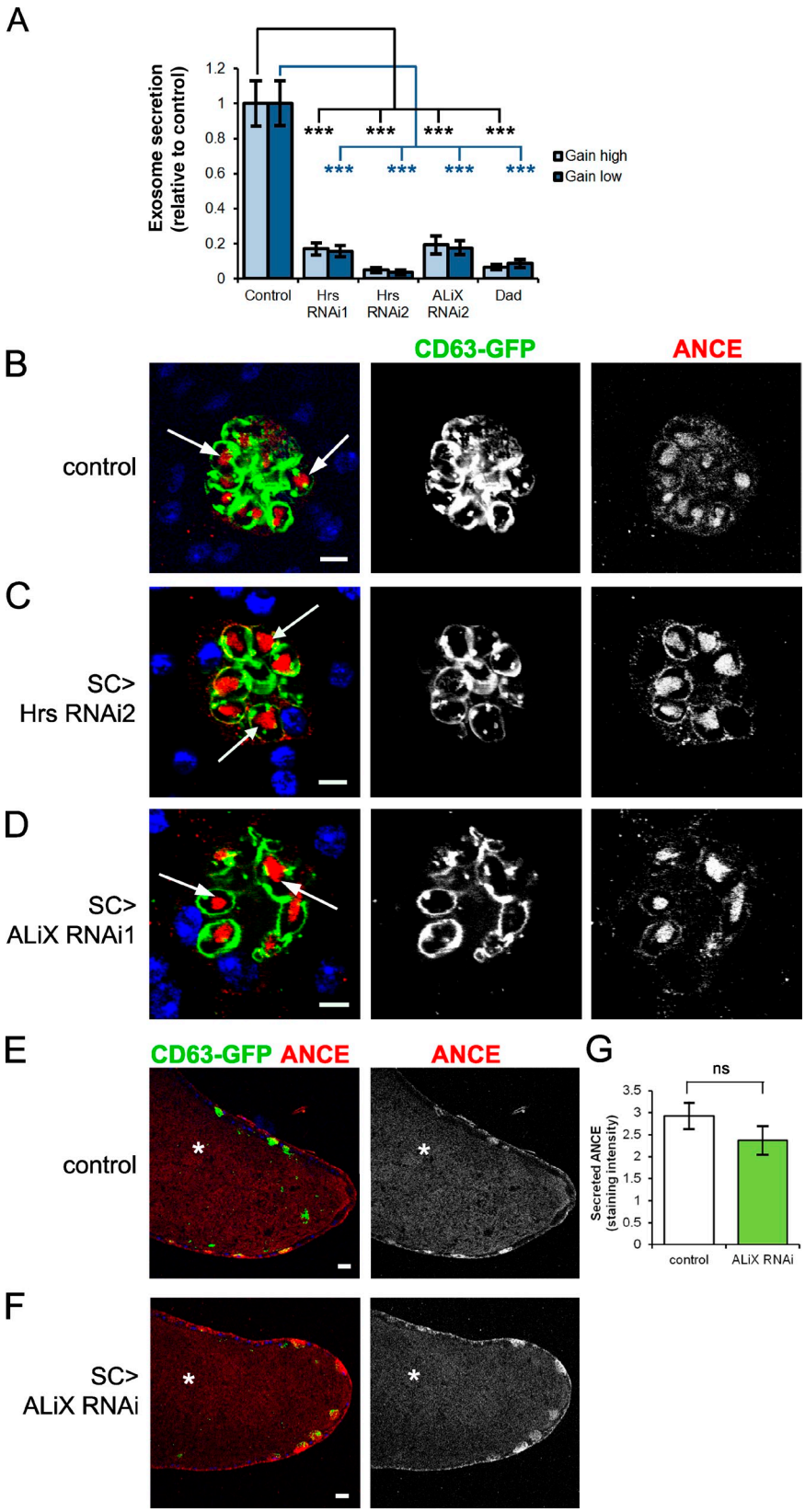

Figure S4. **Blocking ESCRT function in SCs does not affect ANCE secretion.** (A) Relative numbers of SC-expressed CD63-GFP–positive puncta in the AG lumen were quantified for *SC>Hrs-RNAi*, *SC>ALiX-RNAi*, and *SC>Dad* males compared with control males at two confocal gain settings that altered absolute counts by approximately twofold. No effect on relative levels was observed. (B–E) ANCE, which normally localizes to the dense core of control SC SVs (B, arrows) and is secreted into the gland lumen (E, asterisks) but is not detectably expressed in MCs, does not show altered subcellular localization in *Hrs-RNAi*– or *ALiX-RNAi*–expressing SCs (C and D, respectively, arrows). DAPI stains nuclei (blue). (E–G) There is no significant difference in the level of diffuse staining for ANCE in the AG lumen (E and F, asterisks) when *ALiX* is knocked down in SCs (F and G), as measured by calculating the mean signal intensities of three stacked confocal images from the AG lumen taken at 5-µm intervals. Control and *SC>ALiX-RNAi* males were subjected to the same mating protocol as in A, whereas B–D were obtained from virgin males. Data in A and G were analyzed using an unpaired two-tailed Student's *t* test (***, $P < 0.001$, $n > 11$) after the Shapiro–Wilk test to confirm normality. Error bars indicate ±SE. Bars: (B–D) 5 µm; (E and F) 20 µm.

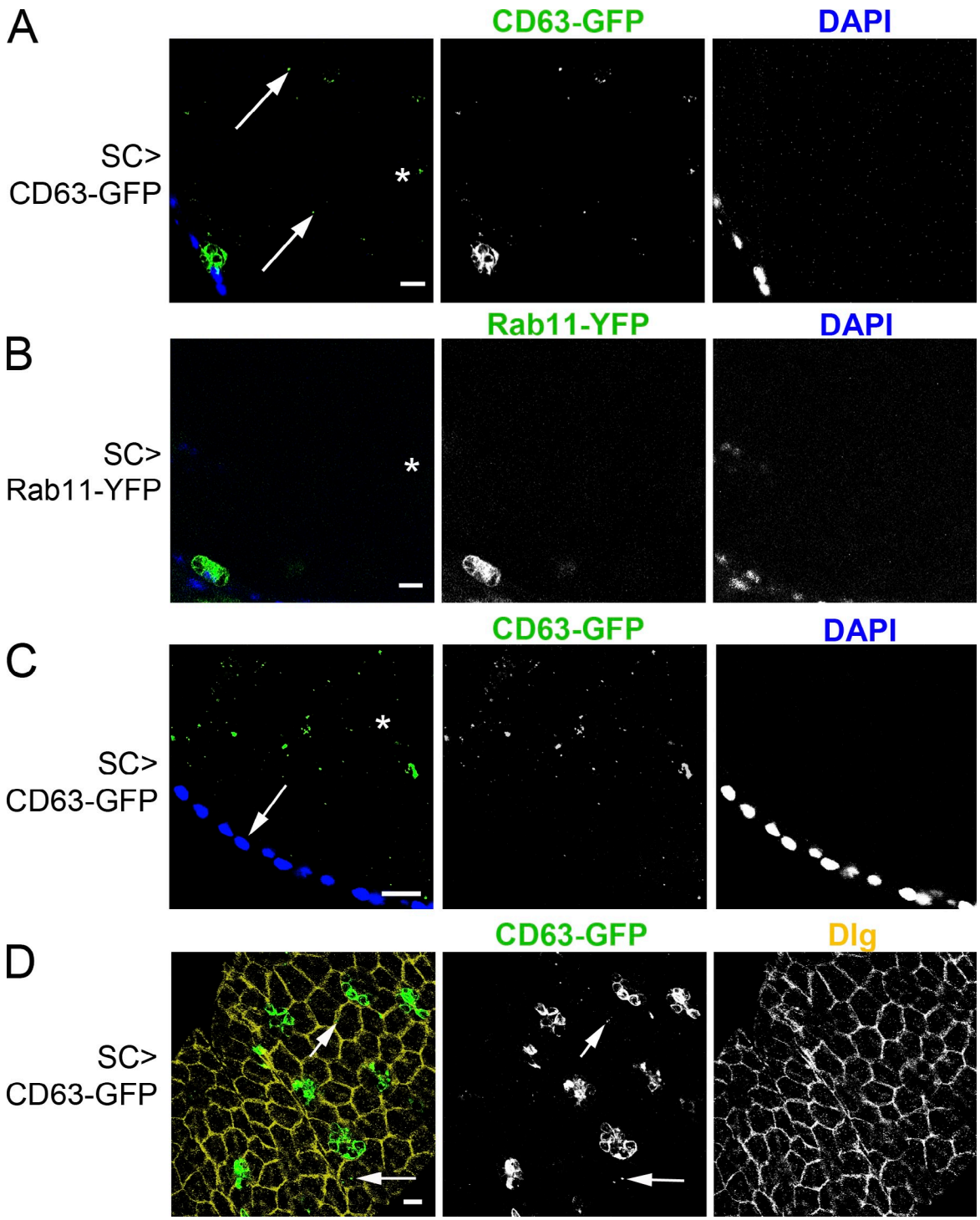

Figure S5. **SC-specific CD63-GFP is transferred to neighboring MCs, but Rab11-YFP is not secreted.** (A and B) Analysis of Rab11-YFP and CD63-GFP secretion when expressed in SCs. Unlike CD63-GFP (A, arrows), YFP-tagged Rab11 is not secreted by SCs, even when highly overexpressed under GAL4 control (B). Images show transverse sections including the lumen (A and B, asterisks) and SCs from 3-d-old males. (C) Transverse section showing no obvious interaction can be seen between CD63-GFP–positive exosomes and the apical surface of MCs (arrow; the asterisk marks the lumen) in most of the AG at 3 d. (D) However, GFP is internalized by the MCs surrounding SCs (arrows). discs large (Dlg) marks apically positioned lateral septate junctions between MCs (junctions between MCs and larger SCs are more apical). DAPI stains nuclei. Bars, 10 µm.

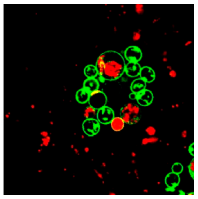

Video 1. **Acidic mMVBLs fuse to nonacidic SVs in SCs.** SC from a 2-d-old male expressing CD63-GFP (green) and stained with LysoTracker red was imaged by time-lapse confocal microscopy using a laser-scanning confocal microscope (LSM 510; Carl Zeiss). Frames were taken every 13.6 s. Stills from this video are shown in Fig. 4 A. Video was produced over a 5-min period. Note how CD63-GFP appears to be transferred to the limiting membrane of the mMVBL at the moment of fusion.

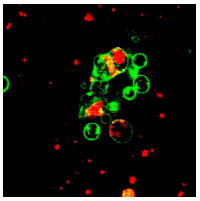

Video 2. **mMVBLs contain CD63-GFP–positive invaginations and acidic microdomains inside mMVBLs.** SC from a 2-d-old male expressing CD63-GFP (green) and stained with LysoTracker red was imaged by time-lapse confocal microscopy using a laser-scanning confocal microscope (LSM 510; Carl Zeiss). Frames were taken every 16.3 s. Stills from this video are shown in Fig. 4 B. Note one CD63-GFP–positive invagination appears to form an ILV-like punctum. A line of peripheral acidic microdomains appears after this event either de novo or through imaging a slightly different plane of the section in the mMVBL. The video was produced over a 5-min period.

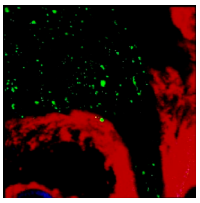

Video 3. **CD63-GFP exosomes may fuse with unmarked sperm tails in females.** Rotating 3D projection of a confocal z stack including the image shown in Fig. 6 D. A z series was collected using a laser-scanning confocal microscope (LSM 510; Carl Zeiss) and the rotating 3D projection movie was recorded using ImageJ 3D Viewer. Note the presence of extended strands of GFP fluorescence and some parallel pairs of short GFP-positive lines that presumably surround sperm tails to which exosomes have recently fused (marked in Fig. 6 D). The female reproductive tract epithelium is marked with CD8-RFP.

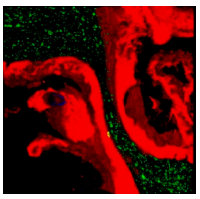

Video 4. **Accumulation of CD63-GFP exosomes along the surface of the female reproductive tract epithelium.** Rotating 3D projection of a confocal z stack including the image shown in Fig. 7 B, highlighting a single GFP-positive interaction site at the epithelial surface that is marked in this figure. A z series was collected using a laser-scanning confocal microscope (LSM 510; Carl Zeiss), and the rotating 3D projection video was recorded using ImageJ 3D Viewer. The female reproductive tract epithelium is marked with CD8-RFP.

Reference

Burgess, J., L.M. Del Bel, C.-I.J. Ma, B. Barylko, G. Polevoy, J. Rollins, J.P. Albanesi, H. Krämer, and J.A. Brill. 2012. Type II phosphatidylinositol 4-kinase regulates trafficking of secretory granule proteins in *Drosophila*. *Development*. 139:3040–3050. http://dx.doi.org/10.1242/dev.077644